Outcomes of Laser Peripheral Iridotomy in Angle Closure Subgroups According to Anterior Segment Optical Coherence Tomography Parameters

Seungbong Han,[1] Kyung Rim Sung,[2] Kyoung Sub Lee,[2] and Ji Wook Hong[2]

[1]Department of Clinical Epidemiology and Biostatistics, College of Medicine, Asan Medical Center, Seoul, Korea
[2]Department of Ophthalmology, University of Ulsan, College of Medicine, Asan Medical Center, Seoul, Korea

Correspondence: Kyung Rim Sung, Department of Ophthalmology, University of Ulsan, College of Medicine, Asan Medical Center, 388-1 Pungnap-2-dong, Songpa-gu, Seoul, Korea 138-736;
sungeye@gmail.com.

Submitted: May 2, 2014
Accepted: September 13, 2014

Citation: Han S, Sung KR, Lee KS, Hong JW. Outcomes of laser peripheral iridotomy in angle closure subgroups according to anterior segment optical coherence tomography parameters. *Invest Ophthalmol Vis Sci*. 2014;55:6795–6801. DOI:10.1167/iovs.14-14714

Purpose. To investigate the effect of laser peripheral iridotomy (LPI) in subgroups of angle closure eyes based on anterior segment optical coherence tomography (AS OCT)-derived parameters.

Methods. Angle closure (primary angle closure [PAC] or PAC glaucoma [PACG]) eyes were imaged using AS OCT before and 2 weeks after LPI. A hierarchical cluster analysis was performed using AS OCT parameters obtained before LPI, such as anterior chamber depth (ACD), anterior chamber width (ACW), iris cross-sectional area (IA), angle opening distance and iris thickness at 750 μm from the scleral spur (AOD_{750}, IT_{750}), iris curvature (IC), lens vault (LV), and anterior chamber area (ACA) to subclassify angle closure eyes. After LPI, parameters were compared to evaluate whether the outcome of LPI differed among the subgroups determined by cluster analysis.

Results. Cluster analysis generated two distinct clusters showing significantly different anatomical features. Cluster 1 (61 eyes) had lower ACD ($P < 0.001$), higher LV ($P = 0.008$), lower AOD_{750} ($P < 0.001$), and lower ACW ($P < 0.001$) than cluster 2 (27 eyes). The proportional change in AOD_{750} after LPI was significantly greater in cluster 1 than in cluster 2 (116.4 ± 117.3% and 46.4 ± 45.7%, respectively, $P = 0.007$).

Conclusions. The outcomes of LPI differed between angle closure subgroups with different anatomical characteristics. Our results provide evidence that angle closure patients can be grouped according to different anatomical anterior segment features and that the pathogenic mechanism of angle closure may differ among subgroups, suggesting that the treatment and follow-up plan should be customized according to subgroup features.

Keywords: glaucoma, angle closure, pupillary block, laser peripheral iridotomy, AS OCT

Primary angle closure glaucoma (PACG) is a leading cause of blindness worldwide, especially in Asian countries.[1–3] The principal mechanism of primary angle closure (PAC) is pupillary block, which is defined as a resistance of aqueous flow from the posterior chamber to the anterior chamber. Thus, laser peripheral iridotomy (LPI), which relieves pupillary block, is the standard treatment for PAC.[4,5] However, a considerable proportion of PAC eyes treated with LPI develop peripheral anterior synechiae (PAS), show persistent angle closure, and/or have an increase in intraocular pressure (IOP). Therefore, LPI may not be effective in treating all cases of narrow angles.[6–11] Pathogenic mechanisms other than pupillary block, such as forward movement of the lens or plateau iris configuration (PIC), have also been suggested to contribute to PAC.[12–15] These reports suggest that PAC is not a single disease entity caused by one mechanism and thus may be subclassifiable according to different features of patient eyes.

In a previous study, we attempted to classify PAC using anterior segment optical coherence tomography (AS OCT)-derived parameters.[16] The main finding of the study was that PAC can be classified into two subgroups: one with higher anterior chamber depth (ACD) and lower lens vault (LV) and the other with lower ACD and higher LV. Nongpiur et al.[17] performed a similar study and categorized their primary angle closure suspects (PACS) into three subgroups using AS OCT parameters. Thus, it appears that PAC or PACS may be composed of several different disease clusters based on common AS characteristics. We therefore hypothesized that the effect of LPI may differ among subgroups of PAC with different anatomical characteristics. Hence, the aim of the current study was to investigate and compare the effect of LPI in subgroups of angle closure patients classified based on anatomical features measured by AS OCT.

Methods

Subjects

Primary angle closure or PACG patients who visited the glaucoma clinic of Asan Medical Center, Seoul, Korea, were seen by a single glaucoma specialist (KRS) and met the inclusion criteria below were consecutively included in this study based on medical record review. We combined PAC and PACG eyes and defined them as having "angle closure" for our current analysis. The study was approved by the Institutional Review Board of Asan Medical Center and followed the tenets of the Declaration of Helsinki.

All participants underwent a complete ophthalmic examination, including a review of their medical history, measurement of best corrected visual acuity (BCVA), slit-lamp biomicroscopy, Goldmann applanation tonometry, gonioscopy, fundoscopic examination using a 90- or 78-diopter (D) lens, stereoscopic optic disc photography, retinal nerve fiber layer photography, central corneal thickness measurement (DGH-550 instrument; DGH Technology, Inc., Exton, PA, USA), a visual field (VF) test (Humphrey field analyzer, Swedish Interactive Threshold Algorithm [SITA] 24-2; Carl Zeiss Meditec, Dublin, CA, USA), and AS OCT (Visante OCT, ver. 2.0; Carl Zeiss Meditec).

Primary angle closure and PACG were diagnosed by gonioscopic examination. Primary angle closure was considered present when an eye had an occludable angle (appositional contact between the peripheral iris and the posterior trabecular meshwork $> 270°$) and exhibited features indicative of trabecular obstruction by the peripheral iris, such as elevated IOP, the presence of PAS, iris whorling (distortion of radially oriented iris fibers), "glaukomflecken" lens opacity, or excessive pigment deposition on the trabecular surface, but without the development of a glaucomatous optic disc or any VF change.[18] Primary angle closure eyes showing glaucomatous optic disc changes (neuroretinal rim thinning, disc excavation, and/or optic disc hemorrhage attributable to glaucoma) or a glaucomatous VF change (pattern standard deviation $< 5\%$ and values outside the normal limits on the glaucoma hemifield test) were considered to have PACG.[18] Only reliable VF test results (false-positive errors $< 15\%$, false-negative errors $< 15\%$, and fixation loss $< 20\%$) were included in the analysis. Eyes with PAS in the nasal or temporal anterior chamber angle before LPI were excluded. We excluded patients with a history or current use of topical or systemic medications that could affect the angle or the pupillary reflex; those with a history of previous intraocular surgery, including cataract surgery, laser trabeculoplasty, laser iridoplasty, and laser iridotomy; and those unable to fixate prior to AS OCT examination. Also excluded were those with a history of acute PAC, defined by the presence of ocular or periocular pain, nausea or vomiting, and a history of intermittent blurring of vision with haloes; a presenting IOP of more than 30 mm Hg; and the presence of at least three of conjunctival injection, corneal epithelial edema, mid-dilated unreactive pupil, and shallow anterior chamber.[19] Eyes diagnosed with secondary angle closure, such as those with neovascular or uveitic glaucoma, were also excluded.

All eyes were newly diagnosed cases, and AS OCT imaging was performed before starting any glaucoma medication. If both eyes met the inclusion criteria, one eye was randomly selected for analysis.

Gonioscopy

Prior to AS OCT imaging, all patients underwent a slit-lamp examination and gonioscopy, conducted by an independent observer (KRS) who had extensive experience in the performance of such examinations. All eyes were examined using a Sussman lens in a darkened room (0.5 cd/m^2). Both static and dynamic gonioscopy were performed using a Sussman lens, with the eye in the primary gaze position. Indentation gonioscopy was performed to determine whether angle closure was attributable to apposition or to PAS. Care was taken to ensure that light did not fall on the pupil during examinations.

AS OCT Imaging

For all participants, imaging was performed through the nasal and temporal angle (0–180°) using AS OCT (Visante OCT, ver. 2.0), operating in the enhanced AS single mode (scan length 16 mm; 256 A-scans) under the same lighting condition (3.25 cd/m^2) before (baseline) and 2 weeks post LPI by a single well-trained operator. Anterior segment parameters in each image were evaluated by an independent examiner (KSL) who was blinded to all other test results and to the clinical information of the participants. Anterior chamber depth, anterior chamber width (ACW), iris cross-sectional area (IA), iris thickness at 750 μm from the scleral spur (IT_{750}), iris curvature (IC), LV, and anterior chamber area (ACA) were determined using ImageJ software (ver. 1.44; National Institutes of Health, Bethesda, MD, USA). Angle opening distance (AOD_{750}), which was provided by the manufacturer of the AS OCT and defined as the linear distance between the point of the inner corneoscleral wall (750 μm anterior to the scleral spur) and the iris, was also assessed. Image acquisition procedure and analysis methods have been previously described in detail.[16,20–22]

Anterior chamber depth was defined as the distance from the corneal endothelium to the anterior surface of the lens. The scleral spur was defined as the point at which a change in curvature of the inner surface of the angle wall became apparent, often presenting as an inward protrusion of the sclera.[23] After determination of the scleral spur location, IT_{750} was defined as the iris thickness measured at 750 μm from the spur.[24] Iris area was defined as the cross-sectional area of both the nasal and temporal sides. Anterior chamber area was defined as the cross-sectional area bordered at the corneal endothelium and anterior surface of the lens and iris. Iris curvature was defined as the maximum perpendicular distance between the iris pigment epithelium and the line connecting the most peripheral to the most central point of the epithelium.[24] Lens vault was defined as the perpendicular distance between the anterior pole of the crystalline lens and the horizontal line joining the two scleral spurs (ACW).[15,25] Measurement variability was checked prior to full analysis by calculating the intraclass correlation coefficients (ICCs). Intra-examiner ICC values for various AS parameters ranged between 0.933 and 0.951.[16]

Laser Peripheral Iridotomy

Laser peripheral iridotomy was performed in the superior region of the iris (from 10–2 o'clock) by sequential argon and neodymium yttrium aluminum garnet after pretreatment with 2% pilocarpine instilled into the eye 1 hour before LPI. Argon settings of 500- to 1000-mW power with a spot size of 50 μm for a duration of 0.05 seconds and a yttrium–aluminum–garnet setting of 2 to 5 mJ were used. Topical medications that could affect the angle measurement were not prescribed post LPI.

Statistical Analysis

Cluster analysis was used to classify patients into distinct subgroups according to features provided by AS OCT. Cluster analysis is a method of segmenting a collection of patients into clusters such that those within each cluster are more closely related to one another than those assigned to different clusters. Specifically, the partitioning around medoids (PAM) method was used for clustering. Medoids are representative subjects of a cluster whose dissimilarity to members within the cluster is minimal.[26] If k is taken as the prechosen number of clusters, the PAM algorithm is based on the search for k representative medoids among the observations of the data set. After finding a set of k medoids, k clusters are constructed by assigning each observation to the nearest medoid. The aim is to find k representative objects that minimize the sum of the dissimilarities (defined below) of the observations to their closest representative object. Compared to the well-known k-means

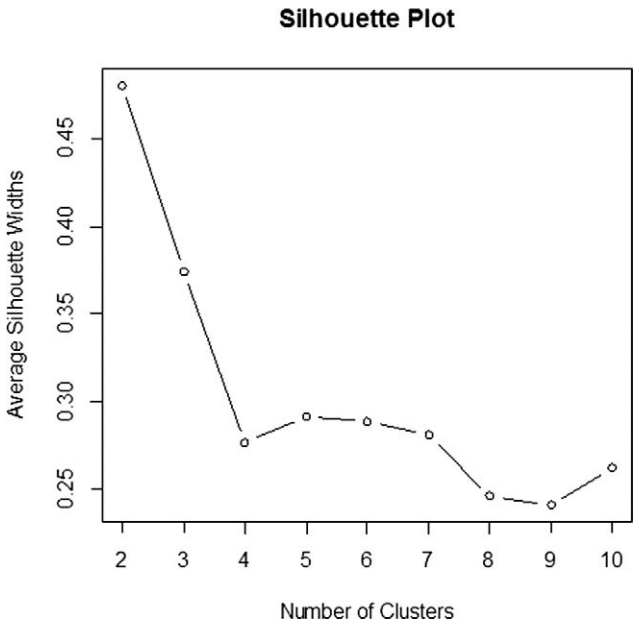

FIGURE 1. Average silhouette widths according to the number of clusters. Euclidean metrics were used.

clustering algorithm, PAM operates on the dissimilarity matrix of the given data set and is more robust on outliers. In addition, it yields a graphical display called a silhouette plot, which permits one to choose the optimal number of clusters.[27] By comparing the overall average silhouette width for each cluster size, we can select the optimal cluster size k to obtain the maximum overall average silhouette width. The silhouette value for each subject represents how appropriate each subject's cluster is. A large silhouette value means that the subject within a certain cluster is well classified. We tried three different dissimilarity metrics, Euclidean, Manhattan, and Gower, and chose the metric that produced the largest overall average silhouette width. Euclidean distances are root sum of squares of differences, and Manhattan distances are the sum of absolute differences. Gower's distance, which was developed by Gower, can be used for non-numeric variables.[28]

The variables used for clustering were ACA, ACD, LV, IC, IA, IT_{750}, AOD_{750}, pupillary distance (PD), and ACW, all of which were obtained by AS OCT before LPI. Parameters were standardized for cluster analysis. After clustering, the above-mentioned parameters were compared between clusters to interpret and characterize the specific clusters. Anterior segment OCT parameters obtained at 2 weeks post LPI and the proportional change in parameters after LPI were compared between clusters to evaluate the outcome of LPI among clusters. Differences were tested by Student's *t*-test or Wilcoxon rank-sum test, and categorical variables were compared with χ^2 statistics or Fisher's exact test. All analyzed variables were compared between PAC and PACG eyes. All statistical analyses were conducted using R software version 2.15.2.[29] To implement the PAM analysis, we used the R package Cluster.[30] All reported *P* values are two-sided, and *P* values less than 0.05 were considered to indicate statistical significance.

RESULTS

A total of 88 angle closure eyes in 88 patients were included in the final analysis. Partitioning around medoids cluster analysis using AS OCT parameters obtained before LPI produced possible clustering structures. Euclidean metrics produced the highest overall silhouette size (0.48) when two clusters were considered (Fig. 1). Other metrics produced smaller maximum overall silhouette widths (Manhattan = 0.4; Gower = 0.22). Therefore, two clusters were generated based on Euclidean metrics. As shown in Figure 2, cluster 1 was more homogeneous than cluster 2.

Among the 88 eyes, 66 had PAC and 22 had PACG. Of the 88, 61 were classified into cluster 1 and 27 eyes into cluster 2.

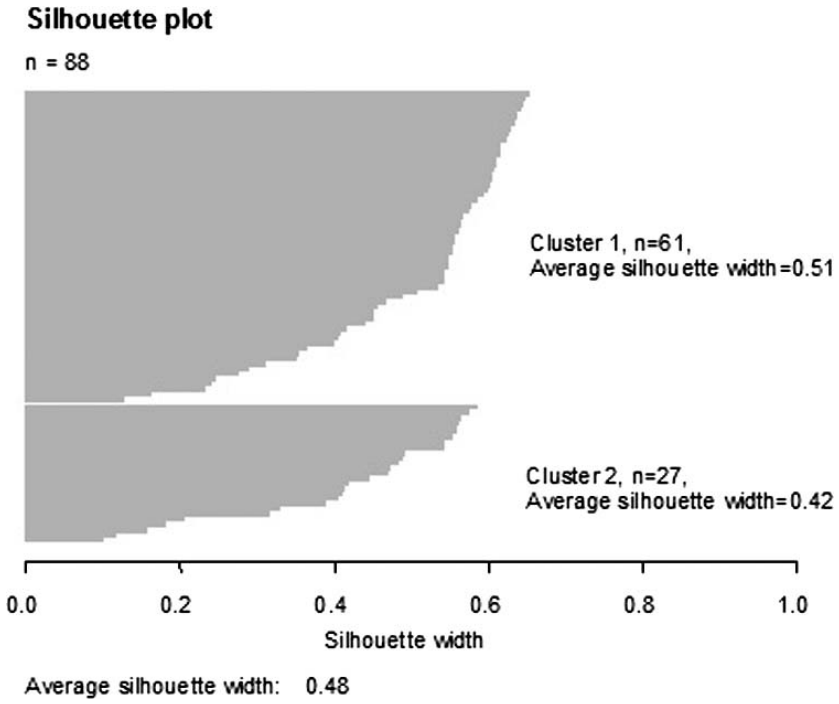

FIGURE 2. Silhouette plot.

Table 1. Comparison of Clinical Characteristics Between the Two Clusters

	Cluster 1, $n = 61$	Cluster 2, $n = 27$	*P* Value
Age, y	62.3 ± 6.9	59.2 ± 6.8	0.053
Sex, male/female	8/53	5/22	0.360
PAC/PACG	46/15	20/7	0.546
SE, diopters	0.91 ± 1.15	0.64 ± 2.27	0.446
BCVA	0.77 ± 0.23	0.86 ± 0.22	0.089
Pre-LPI IOP, mm Hg	16.6 ± 5.1	14.3 ± 2.5	0.030
Post-LPI IOP, mm Hg	14.0 ± 2.8	13.1 ± 2.2	0.184
Post-LPI glaucoma medication, number	0.69 ± 0.81	0.48 ± 0.70	0.252

The mean age (62.3 ± 6.9 and 59.2 ± 6.8 years in clusters 1 and 2, respectively, $P = 0.053$), sex proportion (male/female, 8/53 and 5/22, respectively, $P = 0.360$), PAC/PACG proportion (46/15 and 20/7, respectively, $P = 0.546$), and SE (0.91 ± 1.15 and 0.64 ± 2.27 D, respectively, $P = 0.446$) were not different between the two clusters. Pre-LPI IOP was significantly higher in cluster 1 (16.6 ± 5.1 and 14.3 ± 2.5 mm Hg, respectively, $P = 0.030$), but other parameters such as post-LPI IOP, number of post-LPI glaucoma medications, and BCVA were not different between the two clusters (Table 1).

Anterior segment OCT parameters obtained before LPI were compared between the two clusters (Table 2). Significant differences in anatomical features were found between the two groups. For example, ACA ($P < 0.001$), ACD ($P < 0.001$), AOD_{750} ($P < 0.001$), and ACW ($P < 0.001$) were significantly lower, while LV ($P = 0.008$) was significantly higher in cluster 1 compared to cluster 2.

The AS OCT parameters obtained at 2 weeks post LPI were compared between the two clusters (Table 3). Similar to pre-LPI status, significant differences were seen between groups in terms of ACA, ACD, LV, AOD_{750}, and ACW when assessed at 2 weeks post LPI.

The amount of change and proportional changes (%) in AS parameters after LPI were compared between cluster 1 and 2. Among the analyzed parameters, the proportional change in AOD_{750} after LPI was significantly different between clusters, with a greater change seen in cluster 1 than in cluster 2 (116.4 ± 117.3% and 46.4 ± 45.7%, respectively, $P = 0.007$, Table 4). All other parameters were not significantly different between the two clusters (Table 4).

The amount of change and proportional changes (%) in AS parameters after LPI were compared between PAC and PACG groups. None of them showed significant difference (Table 5).

Figures 3 and 4 show representative cases belonging to cluster 1 and 2, respectively.

Table 2. Comparison of Anterior Segment Optical Coherence Tomography Parameters Obtained Before LPI Between the Two Clusters

	Cluster 1, $n = 61$	Cluster 2, $n = 27$	*P* Value
ACA, mm^2	13.1 ± 1.6	17.8 ± 2.1	<0.001
ACD, mm	1.91 ± 0.19	2.33 ± 0.1	<0.001
LV, mm	1.04 ± 0.28	0.88 ± 0.16	0.008
IC, mm	0.35 ± 0.10	0.32 ± 0.07	0.168
IA, mm^2	1.59 ± 0.29	1.53 ± 0.23	0.375
IT_{750}, mm	0.32 ± 0.09	0.33 ± 0.08	0.170
AOD_{750}, mm	0.14 ± 0.09	0.25 ± 0.09	<0.001
PD, mm	4.18 ± 0.97	4.55 ± 0.69	0.124
ACW, mm	11.2 ± 0.47	11.7 ± 0.40	<0.001

Table 3. Comparison of Anterior Segment Optical Coherence Tomography Parameters Obtained 2 Weeks Post LPI Between the Two Clusters

	Cluster 1, $n = 61$	Cluster 2, $n = 27$	*P* Value
ACA, mm^2	14.2 ± 1.5	18.6 ± 1.8	<0.001
ACD, mm	1.92 ± 0.20	2.32 ± 0.19	<0.001
LV, mm	1.09 ± 0.27	0.89 ± 0.22	0.003
IC, mm	0.12 ± 0.05	0.12 ± 0.05	0.687
IA, mm^2	1.74 ± 0.49	1.71 ± 0.33	0.971
IT_{750}, mm	0.33 ± 0.08	0.33 ± 0.08	0.711
AOD_{750}, mm	0.27 ± 0.12	0.36 ± 0.12	0.003
PD, mm	4.04 ± 0.98	4.14 ± 0.81	0.835
ACW, mm	11.4 ± 0.38	11.7 ± 0.39	<0.001

Discussion

Similar to the results of our previous study, the current cluster analysis generated two clusters of angle closure eyes with completely different pre-LPI anatomical characteristics. One cluster was characterized by shallower ACD and higher LV and the other by relatively deeper ACD and less LV. We added AOD_{750} as another variable in our current analysis. Cluster 1 showed relatively less AOD_{750} than cluster 2. Nongpiur et al.[17] reported that their PACS subjects could be grouped into three clusters. The difference in the number of clusters between their study and ours may reflect our inclusion of PAC/PACG eyes; their patients were PACS only. However, two of the clusters in their analysis showed similar features, such as the difference in ACD, to our two clusters, while their third cluster had mixed features of the other two clusters; therefore, we believe our results are in agreement with theirs. Thus, it appears that angle closure eyes in Asian patients can be grouped into two distinct anatomical types, one with shallower ACD and higher LV, and the other with relatively deeper ACD and lower LV. Additionally, cluster 1 showed smaller ACW compared with cluster 2. Anterior chamber width has been reported as a risk factor in narrow angles.[25] Our result also revealed that eyes in cluster 1 that had narrower angles had smaller ACW. Anterior chamber width is known to have a relationship with ACA or anterior chamber volume.[31] The mean age of the subjects of cluster 1 was slightly older than that of cluster 2. Mean pre-LPI IOP was higher in cluster 1. However, other parameters such as IC or IT were not significantly different between the two clusters. Since the most striking differences between the clusters were ACD and LV, and given that ACD is dependent on LV, we can speculate that the higher LV in cluster 1 may play an important role in the mechanism of angle closure in those patients. Furthermore, aging is reported to significantly increase LV.[22] This effect may result from induction of the forward movement of the lens due to zonular laxity or increases in lens thickness, which can cause an elevated LV. The observation that mean age was slightly greater in cluster 1 may suggest that the increase in LV could contribute to angle closure in cluster 1. Increased LV can directly induce narrowing of the peripheral angle or increase pupillary block by expanding iridolenticular contact. The observation that the change in AOD_{750} after LPI was greater in cluster 1 than in cluster 2 indicates that higher LV and the subsequent increase in pupillary block in cluster 1 significantly improved after LPI. Cluster 2 showed relatively deeper central ACD, and since a clinical feature of PIC is a relatively deeper central ACD, we can speculate that PIC contributes to a pathogenic mechanism of angle closure in the cluster 2 patients. Plateau iris configuration is also characterized as persistent iridotrabecular contact in the presence of patent

Table 4. Mean Difference of Anterior Segment Optical Coherence Tomography Parameters Between Pre and Post LPI and Proportional Change (%) After LPI Compared Between the Two Clusters

	Mean Difference			Proportional Change, %		
	Cluster 1, $n = 61$	Cluster 2, $n = 27$	*P* Value	Cluster 1, $n = 61$	Cluster 2, $n = 27$	*P* Value
ACA, mm^2	1.11 ± 1.08	0.78 ± 1.61	0.326	9.2 ± 9.8	5.0 ± 9.2	0.066
ACD, mm	0.009 ± 0.074	0.008 ± 0.058	0.571	0.5 ± 4.0	0.3 ± 2.5	0.486
LV, mm	0.055 ± 0.208	0.155 ± 0.110	0.606	8.3 ± 23.7	0.9 ± 14.1	0.478
IC, mm	−0.238 ± 0.098	−0.200 ± 0.080	0.055	−65.1 ± 19.9	−61.3 ± 15.2	0.179
IA, mm^2	0.153 ± 0.47	0.176 ± 0.227	0.260	11.3 ± 30.4	11.8 ± 14.3	0.234
IT_{750}, mm	0.011 ± 0.073	−0.008 ± 0.055	0.238	7.0 ± 25.5	1.7 ± 15.9	0.220
AOD_{750}, mm	0.121 ± 0.095	0.104 ± 0.084	0.455	116.4 ± 117.3	46.4 ± 45.7	0.007
PD, mm	−0.15 ± 1.1	−0.42 ± 0.59	0.124	2.3 ± 42.2	9.1 ± 12.8	0.168
ACW, mm	0.14 ± 0.42	0.01 ± 0.33	0.239	1.3 ± 3.8	0.1 ± 2.8	0.238

Table 5. Mean Difference of Anterior Segment Optical Coherence Tomography Parameters Between Pre and Post LPI and Proportional Change (%) After LPI Compared Between the PAC and PACG Groups

	Mean Difference			Proportional Change, %		
	PAC, $n = 66$	PACG, $n = 22$	*P* Value	PAC, $n = 66$	PACG, $n = 22$	*P* Value
ACA, mm^2	0.88 ± 1.19	1.39 ± 1.42	0.214	6.94 ± 9.28	10.8 ± 10.9	0.217
ACD, mm	−0.0003 ± 0.072	0.0350 ± 0.053	0.060	−0.05 ± 3.61	1.95 ± 3.15	0.063
LV, mm	0.045 ± 0.170	0.034 ± 0.226	0.810	6.4 ± 20.6	5.08 ± 24.1	0.700
IC, mm	−0.229 ± 0.089	−0.220 ± 0.109	0.962	−64.9 ± 13.8	−61.0 ± 28.8	0.870
IA, mm^2	0.176 ± 0.454	0.112 ± 0.232	0.560	12.8 ± 29.3	7.4 ± 14.7	0.476
IT_{750}, mm	0.009 ± 0.070	−0.005 ± 0.064	0.362	5.7 ± 24.1	0.11 ± 20.5	0.357
AOD_{750}, mm	0.12 ± 0.091	0.106 ± 0.093	0.547	96.3 ± 110.8	90.8 ± 90.8	0.992
PD, mm	−0.254 ± 0.952	−0.162 ± 1.03	0.965	−1.13 ± 38.6	−1.50 ± 28.5	0.870
ACW, mm	0.057 ± 0.386	0.226 ± 0.421	0.073	0.60 ± 3.44	2.07 ± 3.79	0.075

LPI. Considering that ACD was relatively deeper and the LPI effect relatively smaller in cluster 2, PIC may play some role in angle closure in cluster 2. However, PIC is known to have features like anteriorly directed ciliary process, flat iris plane, and angular insertion of iris; and some of those characteristics are difficult to evaluate by AS OCT.[13,14] Especially ciliary body configuration is not sufficiently assessed in AS OCT. Therefore, our speculation warrants further investigation.

When we compared the degree of change of parameters after LPI between the two clusters, the change in AOD_{750} was found to be significantly different between clusters, indicating that angle opening after LPI was more pronounced in cluster 1 (Figs. 3, 4). Therefore, if we consider the change in AOD_{750} as an effect of LPI, LPI appears to be less effective in the cluster 2 patients. Laser peripheral iridotomy is intended to resolve pupillary block; therefore, if LPI is not effective in resolving angle closure, the contribution of pupillary block to angle closure is likely to be less in those eyes. Under this assumption, the role of pupillary block in angle closure in eyes of cluster 2 may be small. In other words, a mechanism other than pupillary block may contribute to angle closure in eyes of cluster 2. Alternatively, our findings may indicate that cluster 2 had a relatively greater AOD_{750} at baseline, and thus the

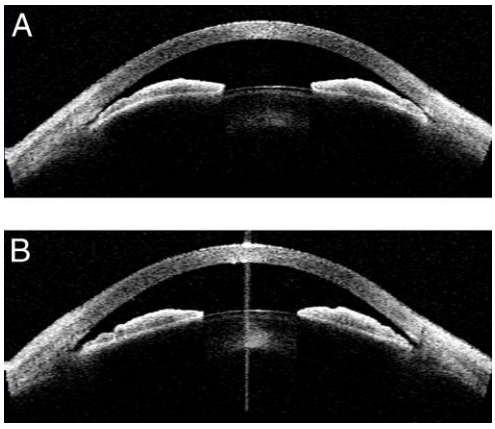

Figure 3. Representative case belonging to cluster 1. (**A**) Anterior segment OCT image with relatively lower ACD (1.64 mm) and higher LV (1.3 mm) at pre LPI. This eye showed greater AOD_{750} change (255.8%) after LPI (**B**).

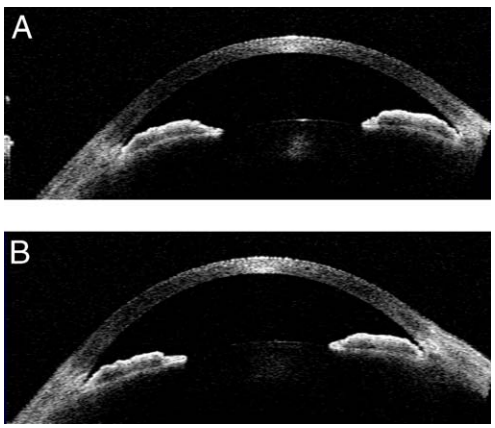

Figure 4. Representative case belonging to cluster 2. (**A**) Image of eye with relatively higher ACD (2.20 mm) and lower LV (0.95 mm). (**B**) A small amount of AOD_{750} change (64.4%) after LPI.

proportional change in AOD_{750} was less than that of cluster 1. Mean difference of AOD_{750} between pre and post LPI was not significantly different between the two clusters.

Our study has several limitations. Our subclassification of angle closure did not consider dynamic features. Since not all eyes with narrow angles develop angle closure, dynamic features may also contribute to angle closure.[21,32–36] Furthermore, as mentioned earlier, current AS OCT is unable to visualize the structures behind the iris. Inclusion of other parameters related to ciliary body location and the relationship between ciliary body and iris root may be helpful to subclassify angle closure eyes according to the parameters provided by AS OCT. Angle closure may not be caused by single pathogenic mechanism in specific eyes. For instance, pupillary block and PIC may contribute to angle closure at the same time. Thus, the possibility that angle closure can be induced by a complex mechanism should be also considered.

In conclusion, the outcome of LPI differed among subgroups of angle closure eyes based on anatomical characteristics. Our results provide evidence that PAC is composed of subgroups with different anatomical anterior segment features and therefore with distinct pathogenic mechanisms underlying angle closure. Treatment and follow-up plans should be customized for each patient subgroup.

Acknowledgments

The authors have no proprietary interests in or financial support for the development or marketing of instruments or equipment mentioned in this article or any competing instruments or equipment.

Disclosure: **S. Han**, None; **K.R. Sung**, None; **K.S. Lee**, None; **J.W. Hong**, None

References

1. Congdon N, Wang F, Tielsch JM. Issues in the epidemiology and population-based screening of primary angle-closure glaucoma. *Surv Ophthalmol*. 1992;26:411–423.
2. Foster PJ, Baasanhu J, Alsbirk PH. Glaucoma in Mongolia: a population-based survey in Hovsgol province, northern Mongolia. *Arch Ophthalmol*. 1996;114:1235–1241.
3. Foster PJ, Johnson GJ. Glaucoma in China: how big is the problem? *Br J Ophthalmol*. 2001;85:1277–1282.
4. Saw SM, Gazzard G, Friedman DS. Interventions for angle-closure glaucoma: an evidence-based update. *Ophthalmology*. 2003;110:1869–1878.
5. Nolan WP, Foster PJ, Devereux JG, et al. YAG laser iridotomy treatment for primary angle closure in east Asian eyes. *Br J Ophthalmol*. 2000;84:1255–1259.
6. Alsagoff Z, Aung T, Ang LP, et al. Long-term clinical course of primary angle-closure glaucoma in an Asian population. *Ophthalmology*. 2000;107:2300–2304.
7. He M, Friedman DS, Ge J, et al. Laser peripheral iridotomy in primary angle-closure suspects: biometric and gonioscopic outcomes: the Liwan Eye Study. *Ophthalmology*. 2007;114:494–500.
8. Lee KS, Sung KR, Kang SY, et al. Residual anterior chamber angle closure in narrow-angle eyes following laser peripheral iridotomy: anterior segment optical coherence tomography quantitative study. *Jpn J Ophthalmol*. 2011;55:213–219.
9. Aung T, Ang LP, Chan SP, Chew PT. Acute primary angle-closure: long-term intraocular pressure outcome in Asian eyes. *Am J Ophthalmol*. 2001;131:7–12.
10. Ang LP, Aung T, Chew PT. Acute primary angle closure in an Asian population: long-term outcome of the fellow eye after prophylactic laser peripheral iridotomy. *Ophthalmology*. 2000;107:2092–2096.
11. Choi JS, Kim YY. Progression of peripheral anterior synechiae after laser iridotomy. *Am J Ophthalmol*. 2005;140:1125–1127.
12. He M, Foster PJ, Johnson GJ, et al. Angle-closure glaucoma in East Asian and European people. Different diseases? *Eye*. 2006;20:3–12.
13. Kumar RS, Baskaran M, Chew PT, et al. Prevalence of plateau iris in primary angle closure suspects: an ultrasound biomicroscopy study. *Ophthalmology*. 2008;115:430–434.
14. Kumar RS, Tantisevi V, Wong MH, et al. Plateau iris in Asian subjects with primary angle closure glaucoma. *Arch Ophthalmol*. 2009;127:1269–1272.
15. Nongpiur ME, He MG, Amerasinghe N, et al. Lens vault, thickness and position in Chinese subjects with angle closure. *Ophthalmology*. 2011;118:474–479.
16. Baek S, Sung KR, Sun JH, et al. A hierarchical cluster analysis of primary angle closure classification using anterior segment optical coherence tomography parameters. *Invest Ophthalmol Vis Sci*. 2013;54:848–853.
17. Nongpiur ME, Gong T, Lee HK, et al. Subgrouping of primary angle-closure suspects based on anterior segment optical coherence tomography parameters. *Ophthalmology*. 2013;120:2525–2531.
18. Foster PJ, Buhrmann R, Quigley HA, et al. The definition and classification of glaucoma in prevalence surveys. *Br J Ophthalmol*. 2002;86:238–242.
19. Lee KY, Rensch F, Aung T, et al. Peripapillary atrophy after acute primary angle closure. *Br J Ophthalmol*. 2007;91:1059–1061.
20. Lee KS, Sung KR, Shon K, et al. Longitudinal changes in anterior segment parameters after laser peripheral iridotomy assessed by anterior segment optical coherence tomography. *Invest Ophthalmol Vis Sci*. 2013;54:3166–3170.
21. Lee Y, Sung KR, Na JH, et al. Dynamic changes in anterior segment (AS) parameters in eyes with primary angle closure (PAC) and PAC glaucoma and open-angle eyes assessed using AS optical coherence tomography. *Invest Ophthalmol Vis Sci*. 2012;53:693–697.
22. Sun JH, Sung KR, Yun SC, et al. Factors associated with anterior chamber narrowing with age: an optical coherence tomography study. *Invest Ophthalmol Vis Sci*. 2012;53:2607–2610.
23. Sakata LM, Lavanya R, Friedman DS, et al. Assessment of the scleral spur in anterior segment optical coherence tomography images. *Arch Ophthalmol*. 2008;126:181–185.
24. Wang B, Sakata LM, Friedman DS, et al. Quantitative iris parameters and association with narrow angles. *Ophthalmology*. 2010;117:11–17.
25. Nongpiur ME, Sakata LM, Friedman DS, et al. Novel association of smaller anterior chamber width with angle closure in Singaporeans. *Ophthalmology*. 2010;117:1967–1973.
26. Hastie T, Tibshirani R, Friedman J. *The Elements of Statistical Learning: Data Mining, Inference and Prediction*. New York, NY: Springer; 2001.
27. Kaufman L, Rousseeuw PJ. *Finding Groups in Data: An Introduction to Cluster Analysis*. *Wiley Series in Probability and Mathematical Statistics*. Hoboken, NJ: Wiley; 1990.
28. Gower JC. A general coefficient of similarity and some of its properties. *Biometrics*. 1971;27:857–874.
29. R Development Core Team. *R: A Language and Environment for Statistical Computing*. Vienna, Austria: R Foundation for Statistical Computing. Available at: http://www.R-project.org. Accessed April 24, 2014.
30. Maechler M, Rousseeuw P, Struyf A, Hubert M, Hornik K. Cluster: Cluster Analysis Basics and Extensions. R package version 4.4. 2013.

31. Wang D, Qi M, He M, Wu L, Lin S. Ethnic difference of the anterior chamber area and volume and its association with angle width. *Invest Ophthalmol Vis Sci*. 2012;53:3139–3144.
32. Quigley HA, Silver DM, Friedman DS, et al. Iris cross-sectional area decreases with pupil dilation and its dynamic behavior is a risk factor in angle closure. *J Glaucoma*. 2009;18:173–179.
33. Aptel F, Denis P. Optical coherence tomography quantitative analysis of iris volume changes after pharmacologic mydriasis. *Ophthalmology*. 2010;117:3–10.
34. Quigley HA. The iris is a sponge: a cause of angle closure. *Ophthalmology*. 2010;117:1–2.
35. Quigley HA. Angle-closure glaucoma—simpler answers to complex mechanisms: LXVI Edward Jackson Memorial Lecture. *Am J Ophthalmol*. 2009;148:657–669.
36. Leung CK, Cheung CY, Li H, et al. Dynamic analysis of dark-light changes of the anterior chamber angle with anterior segment OCT. *Invest Ophthalmol Vis Sci*. 2007;48:4116–4122.

Investigative Ophthalmology & Visual Science